

# Upper Barremian–lower Aptian charophyte biostratigraphy from Arrifes section (Algarve Basin, Southern Portugal): correlation with dinoflagellate cyst biostratigraphy

Jordi Pérez-Cano <sup>a, b, c, d, \*</sup>, Hélder J.R. Pereira <sup>e, f</sup>, Marcia Mendes <sup>g</sup>, Zélia Pereira <sup>g</sup>,  
Pedro Miguel Callapez <sup>e, h</sup>, Paulo Fernandes <sup>f</sup>

<sup>a</sup> Institut Català de Paleontologia Miquel Crusafont, Universitat Autònoma de Barcelona, ICTA-ICP Building, c/de les Columnes s/n, Campus de la UAB, Cerdanyola del Vallès, Catalonia E-08193, Spain

<sup>b</sup> Departament de Dinàmica de la Terra i de l'Oceà, Facultat de Ciències de la Terra, Universitat de Barcelona-UB, Barcelona, Catalonia 08028, Spain

<sup>c</sup> Institut de Recerca de la Biodiversitat (IRBio), Universitat de Barcelona (UB), Barcelona, Spain

<sup>d</sup> Departament de Mineralogia, Petrologia i Geologia Aplicada, Facultat de Ciències de la Terra, Universitat de Barcelona-UB, Barcelona, Catalonia 08028, Spain

<sup>e</sup> Centre for Earth and Space Research of the University of Coimbra (CITEUC), Faculty of Sciences and Technology, Earth Sciences Department, University of Coimbra – Pólo II, Rua Sílvio Lima, Coimbra 3030–790, Portugal

<sup>f</sup> CIMA, Centre of Marine and Environmental Research||ARNET – Infrastructure Network in Aquatic Research, University of Algarve, Campus de Gambelas, Faro 8000-139, Portugal

<sup>g</sup> LNEG, National Laboratory of Energy and Geology, Rua da Amieira, S. Mamede de Infesta 4465-965, Portugal

<sup>h</sup> Grupo de Investigación Paleolbérica, Departamento de Geología y Geografía, Universidad de Alcalá, Alcalá de Henares 28871, Spain

## ARTICLE INFO

### Article history:

Received 14 February 2023

Received in revised form

18 April 2023

Accepted in revised form 5 May 2023

Available online 18 May 2023

### Keywords:

Charophyta

Iberia

Cretaceous

Clavatoraceae

Continental-marine biochronology

Palynology

## ABSTRACT

The Arrifes section (Algarve Basin, Southern Portugal) has been studied from the viewpoint of charophyte biostratigraphy. The previous sedimentological studies in this section showed that it is built of the interbedding of continental and marine facies that contain both marine and continental palynomorphs (pollen, spores, and dinoflagellates), providing an excellent sedimentary context to perform direct correlations between marine and continental domains. In the present work, the identified charophyte biozones have been correlated with dinoflagellate biozones previously recognized in the Arrifes section, being the first time that these two biochronologies can be directly correlated. From the charophyte biostratigraphy viewpoint, two assemblages are distinguished. The older one is found between 65 and 135 m of the stratigraphic section, and it is composed of the species *Echinocara lazarii*, *Atopochara trivolvii* var. *trivolvii*, *Clavator grovesii* var. *jiuquanensis*, *Clavator harrisii* var. *harrisii*, *C. harrisii* var. *reysi*, and *C. harrisii* var. *zavialensis*. This assemblage belongs to the upper Barremian–lower Aptian *Clavator grovesii* var. *jiuquanensis* Eurasian biozone and also to the *Asciidiella cruciata*–*Pseudoglobator paucibracteatus* European biozone and it is described in beds with the dinoflagellate cyst *Subtilisphaera scabrata* (lower to lowermost upper Barremian) and *Odontochitina operculata* (from upper Barremian upwards). The younger charophyte assemblage is found between 135 and 155 m of the stratigraphic section, and it is composed of the species *A. trivolvii* var. *trivolvii*, *Clavator grovesii* var. *corrugatus*, *Clavator harrisii* var. *harrisii*, *C. harrisii* var. *reysi*, and *C. harrisii* var. *zavialensis*. This assemblage belongs to *Clavator grovesii* var. *corrugatus* biozone, previously assigned to upper Aptian (*Clavator grovesii* var. *lusitanicus* biozone). However, in the Arrifes section, this assemblage is found in beds assigned to the dinoflagellate cyst *Odontochitina operculata* (from upper Barremian–lower Aptian). The direct correlation of the base of the *C. grovesii* var. *corrugatus* biozone with the dinoflagellate cyst *O. operculata*, indicates that the base of the *Clavator grovesii* var. *corrugatus* biozone is in the upper lower Aptian, which is slightly older than was previously suggested, and it is extended until the middle Albian.

© 2023 The Author(s). Published by Elsevier Ltd. This is an open access article under the CC BY license (<http://creativecommons.org/licenses/by/4.0/>).

\* Corresponding author. Institut Català de Paleontologia Miquel Crusafont, Universitat Autònoma de Barcelona, ICTA-ICP Building, c/de les Columnes s/n, Campus de la UAB, Cerdanyola del Vallès E-08193, Catalonia, Spain.

E-mail addresses: [jordi.perez@icp.cat](mailto:jordi.perez@icp.cat), [jordi\\_perez-cano@ub.edu](mailto:jordi_perez-cano@ub.edu) (J. Pérez-Cano).

## 1. Introduction

Charophyte fructifications (utricle) of the Clavatoraceae family are one of the main fossil groups used for the biostratigraphic characterization of Lower Cretaceous continental record (e.g., Grambast, 1974; Rey and Ramalho, 1974; Martín-Closas, 1989; Musacchio, 1989, 2000; Schudack, 1993; Trabelsi et al., 2016; Sanjuan et al., 2021). In the last decades, detailed biozonations have been proposed, especially in European and Chinese basins (e.g., Wang and Lu, 1982; Riveline et al., 1996; Mojon, 1996, 2002; Martín-Closas et al., 2009; Pérez-Cano et al., 2022a). However, few data can allow a precise correlation of the charophyte biozonations with the coeval standard marine biozonations, as only in some cases both domains are correlated. Continental-marine correlations can be performed in three different manners. 1) Direct correlations are established when continental and marine fossils are found interbedded or together in the same stratigraphic section or the same bed. 2) Indirect correlations are made after performing a lithostratigraphic equivalence between/among different sections, describing charophytes and marine organisms, respectively. 3) The compilation correlation is the most common type of marine-continental correlation, and it is carried out on a regional scale, using regional geological data, such as sequence stratigraphy or the age of the marine units that overlay and underlay the non-marine ones. The correlation between charophyte biozones with their coeval standard marine biozones for the Lower Cretaceous Series was first summarized by Riveline et al. (1996). In recent years, the correlation has been improved for the Barremian–lower Aptian timespan by establishing direct correlations (e.g., Martín-Closas et al., 2009) or using chemostratigraphic methods, such as Sr-isotope stratigraphy (Pérez-Cano et al., 2022a).

The present work is focused on the upper Barremian–Aptian charophyte biostratigraphy. According to the extant charophyte biozonation, three biozones are described for this stratigraphic interval. The *Asciidiella cruciata*–*Pseudoglobator paucibracteatus* European biozone and the *Clavator grovesii* var. *jiuquanensis* Eurasian biozone are almost equivalent and their ages are upper lower Barremian–lower Aptian and upper Barremian–lower Aptian, respectively (Pérez-Cano et al., 2022a). The *Clavator grovesii* var. *corrugatus* biozone overlies the previous biozones, and its age is considered as late Aptian – middle Albian (Riveline et al., 1996; Pérez-Cano et al., 2022a). However, the boundary between both biozones is usually difficult to describe and correlate with the marine domain due to the recorded marine transgression between the late Barremian–lower Aptian in the Tethyan Realm. This transgression reached its peak point in the early Aptian (e.g., Hardenbol et al., 1998; Wissler et al., 2003; Pictet et al., 2015; Bover-Arnal et al., 2016), restricting the deposition of continental facies to few basins, where both biozones can be found without sedimentary discontinuities (e.g., Trabelsi et al., 2016). The main goal of this work is to improve the correlation and the equivalence between integrated continental and marine biozonations in the upper Barremian–Aptian time interval. The charophyte assemblages from the Arrifes section (Algarve, Southern Portugal) have been studied to achieve this objective. This section is composed of the interbedding of shallow marine to transitional continental marls, limestones, and minor sandstones and conglomerates, which yield a significant diversity of terrestrial and marine palynomorphs, including spores, pollen grains, and dinoflagellate cysts, the latter already used as biostratigraphic markers (Mendes et al., 2023) providing a unique context to establish direct correlations between terrestrial and marine domains. The present work proposes a direct correlation between the charophyte biozones described in the study of charophyte assemblages with the dinoflagellate biozones previously identified by Mendes et al. (2023). This correlation

improves the application, accuracy, and utility of extant upper Barremian–Aptian charophyte biozones.

## 2. Geological setting

The Algarve Basin is located in southernmost Portugal (Fig. 1A), and its sedimentary infilling is composed of rocks that range from the Upper Triassic to the recent (Manuppella et al., 1988; Fernandes et al., 2013; Terrinha et al., 2013). The first sedimentary cycle is of the Late Triassic–earliest Jurassic age corresponding to the initial continental rifting phase of Pangaea breakup in the Iberian range and formation of the Central Atlantic. The latter comprises a succession of continental red beds, followed by evaporites, and is capped by volcano-sedimentary deposits related to the Central Atlantic Magmatic Province (Verati et al., 2007; Vilas-Boas et al., 2022). The following sedimentary cycle consists of Sinemurian to Tithonian shelf carbonates deposited during the passive margin phase (Rocha, 1976; Manuppella et al., 1987; Marques and Rocha, 1988a, 1988b; Azerêdo et al., 2003; Dommergues et al., 2011; Borges et al., 2011, 2012). Changes in the thickness and facies of the carbonate sequences, together with regional unconformities and hiatuses, are attributed either to carbonate allocyclic processes, global sea level variations or regional tectonic events (Manuppella, 1988; Terrinha et al., 2013; Ramos et al., 2016).

The Lower Cretaceous sedimentary interval (Berriasian to Cenomanian) is also included in the passive margin succession. However, it differs from the Jurassic sequences due to its mixed carbonate and siliciclastic composition (Rey, 2006, 2009). Berriasian marls and dolomites are found at the base of the Lower Cretaceous sedimentary interval, and it is upwards followed by Valanginian to Barremian marls, dolomites, sandstones, and mudstones deposited in nearshore and continental settings. The Aptian to lower Albian sedimentary sequences comprise, at the base, variegated mudstones and carbonates of nearshore to lagoonal settings, followed by transgressive marl and limestone cycles. Upper Albian to Cenomanian strata are only known in the eastern Algarve Basin, where they are represented by shallow water carbonate platform limestones interbedded with marls and dolomites. The age determinations of the Lower Cretaceous strata were mostly based on foraminifera biostratigraphy (Rey and Ramalho, 1974; Ramalho and Rey, 1981; Rey, 1983, 1986, 2006; Correia, 1989, 2009) and palynology (Berthou, 1983; Berthou and Leerevel, 1990; Hochuli et al., 2006; Heimhofer, 2007; Mendes et al., 2023).

In the region of Albufeira (Fig. 1B), the Lower Cretaceous carbonates that comprise the Arrifes section can be observed on the subvertical and vertical strata outcropping on the coastal cliffs (Fig. 1C). These strata were deformed due to the tectonic inversion of the Algarve Basin, which caused the compression and the uplift of the nearby Albufeira diapir (Terrinha, 1998; Terrinha et al., 2013; Ramos et al., 2016). The present work follows the most recent sedimentological and age determination, based on dinoflagellates, of the Arrifes section carried out by Mendes et al. (2023). The section probably correlates with the Salema, Barrancão and Burgau Formations (Fig. 1E). However, there is a lateral change between the western part of the Algarve Basin and the Central part, challenging a clear attribution of the succession in the Arrifes section to particular lithostratigraphic units.

## 3. Materials and methods

The Arrifes section is located on the coastal cliffs at the western part of Albufeira; base: 37°04'43.12" N, 8°16'11.10" W; top: 37°04'35.33" N, 8°16'35.54" W (Fig. 1B–C). The section is 194 m thick, and it is mainly composed of marls, limestones, and marly limestones. Sandstones and conglomerates are locally found (Figs. 1C, D and 2). For the present work, between 1 and 3 kg of

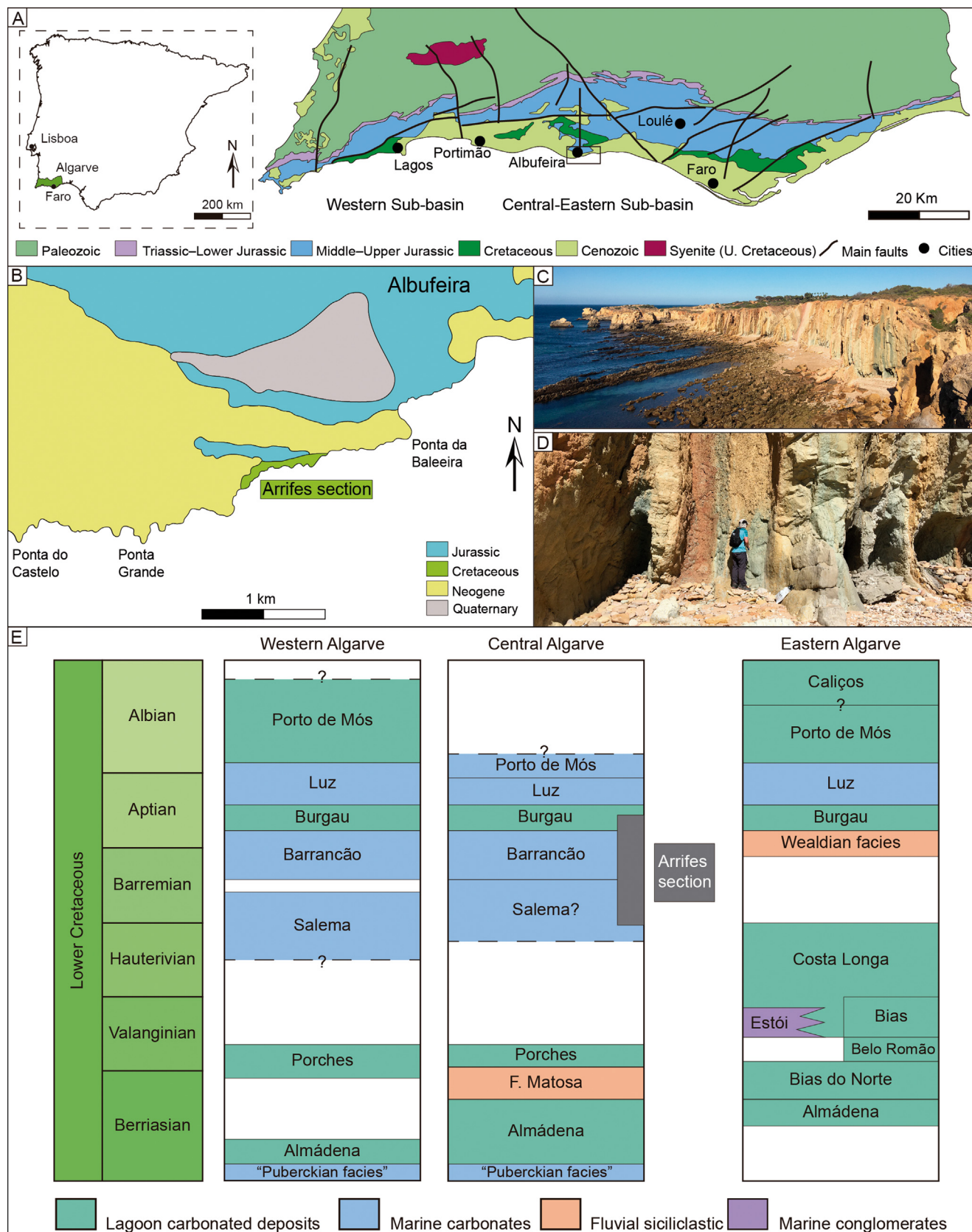


**Fig. 1.** A) Location and geologic map of the Algarve Basin (modified from Oliveira et al., 1992; Manuppella, 1992; Ramos et al., 2016). The squared area corresponds to the zone represented in Fig. 1C. B) Simplified map of the Albufeira region, showing the location of the Arrifes section (modified from Rocha et al., 1989). C) Outcrop of the Arrifes section. D) Detail of the Arrifes section. E) Lithostratigraphy of the Algarve Basin (adapted from Rey, 2006; Terrinha et al., 2013; Mendes et al., 2023) and the stratigraphic interval assigned to the Arrifes section in this study. The assignment of the lithostratigraphic units from the Arrifes section is tentative.



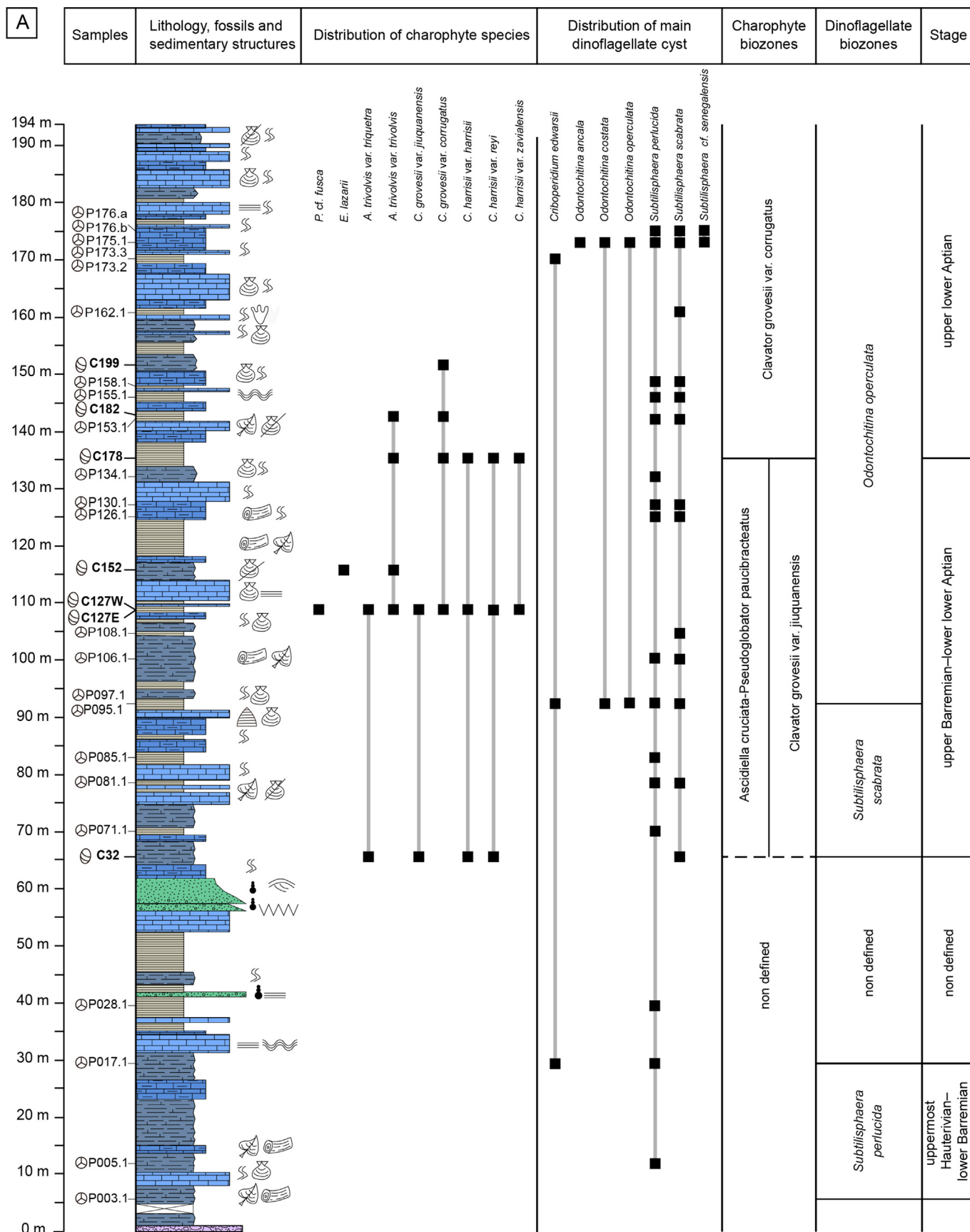


**Fig. 2.** A) Stratigraphic log of Arrifes section with the stratigraphic position of the studied samples, and the charophyte and dinoflagellate cysts biostratigraphy (modified from Mendes et al., 2023). The palynological sample's position and results were provided by Mendes et al. (2023). B) Key to Figure A.

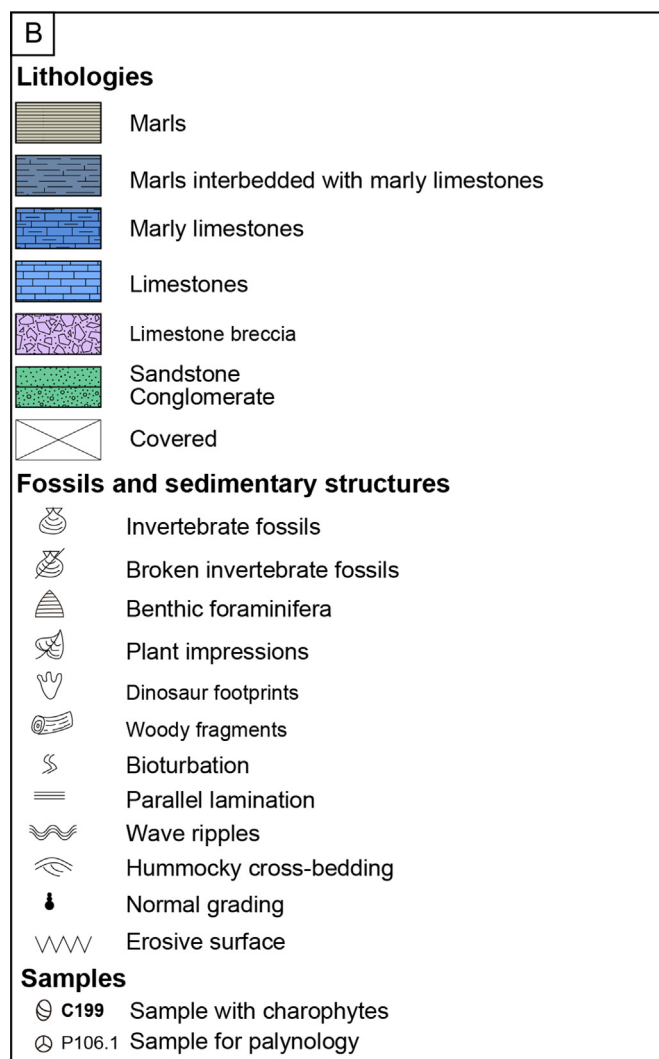


Fig. 2. (continued).

marls were collected from 20 marl beds along the entire section. Samples were prepared in the Palaeontological Laboratory of the Departament de Dinàmica de la Terra i de l'Oceà, Universitat de Barcelona. Each sample was put in a solution of water, oxygen peroxide ( $\text{H}_2\text{O}_2$ ; eliminates the organic matter), and sodium carbonate ( $\text{Na}_2\text{CO}_3$ ; deflocculates the clays). After a few days, the samples were sieved using three meshes of 1000, 500, and 200  $\mu\text{m}$ . Once the samples were dried, the microfossils (including charophytes fructifications and thalli, ostracods, vertebrate remains, and other associated microfossils) were hand-picked using small brushes under a binocular microscope AmScope SE305R-PZ-LED under the magnifications of  $\times 10$ ,  $\times 20$ ,  $\times 30$ , and  $\times 60$ . The picked up charophytes and other fossils are temporarily stored at Institut Català de Paleontologia Miquel Crusafont and will be housed in the Geological Museum of Portugal (Lisbon) once their study is concluded. Figured specimens have provisional references (Arr-Ch-1 to Arr-Ch-37) that will have their equivalence once they are definitively housed. Appendix 1 shows the equivalence of figured specimens with this provisional reference.

#### 4. Systematic charophyte palaeobotany

The taxonomy and systematic discussion of charophytes are not the focus of this study. This topic has been extensively discussed

over the last decades (e.g., Feist and Wang, 1995; reply by Martín-Closas and Schudack, 1997), resulting in the establishment of two different visions, i.e., the phenetic and the cladistic vision. The present study follows the phylogenetic approach developed by Martín-Closas (1989, 1996) and Schudack (1993).

Rey and Ramalho (1974) first described Lower Cretaceous charophytes in the Algarve Basin, particularly in the Barremian–Aptian deposits of the western part of the basin (Burgau and Luz sections). Later, Grambast-Fessard (1980a, 1980b, 1986) described Aptian (and Albian?) charophyte flora also in the western part of the basin (Luz and Zavial sections). These studies enabled the description of *Asciidiella reticulata* var. *irregularis* (Grambast-Fessard, 1986) Martín-Closas 1996, which is, until now, only found in the Algarve.

Charophyte remains in the Arrifes section were found in seven samples, that were gathered in the middle to upper part of the stratigraphic section (Fig. 2). The charophyte assemblage is composed of 11 taxa, including charophyte fructifications and thalli (Figs. 3 and 4; Appendix 2). Most of the recovered charophyte fructifications show superficial erosion and are sometimes broken suggesting lateral transport. Charophyte thalli are very rare and when occur they are very small portions. These taphonomical features of the fructifications and thalli indicate some degree of biostratinomic selection before deposition (see e.g., Vicente et al., 2016; Pérez-Cano et al., 2022b); for that reason, the studied assemblages are usually considered parautochthonous (locally allochthonous), suggesting a short-term transport towards the inner carbonate platform. The abundance of charophyte fructifications in each sample is found in Appendix 2.

##### 4.1. Charophyte fructifications

Division Charophyta Migula, 1897

Class Charophyceae Smith, 1938

Order Charales Lindley, 1836

Family “Porocharaceae” (Grambast, 1962) emend. Schudack, 1993

Genus *Porochara* (Mädler, 1955) emend. Schudack, 1986

Morphogroup *Porochara fusca* sensu Martín-Closas (1989, 2000) and Schudack (1993)

##### *Porochara* cf. *fusca*

Fig. 3A–B

1952 *Aclistochara fusca* nov. sp. – Mädler p. 19–20, Pl. A, figs. 22–25.  
1955 *Porochara fusca* (Mädler 1952) nov. comb. – Mädler, p. 271.

**Description.** Five porocharacean gyrogonites have been found in sample C127W (Appendix 2). They are small (<500  $\mu\text{m}$  height and wide), and ellipsoidal. The base is rounded, and the apex has an apical pore (Fig. 3B). The number of convolutions varies between 8 and 10. The inner part is recrystallized, impeding the observation of the basal plate, and consequently, these gyrogonites could be also attributed to the genus *Feistiella* Schudack, 1986. Nevertheless, they have been assigned to the genus *Porochara* as no *Feistiella* species are described in the Barremian nor the Aptian and there are no *Feistiella* species with a width or length <500  $\mu\text{m}$ . The species assignation remains as ‘coffer to’, as the number of gyrogonites is very low to make a clear morphometric analysis and identification.

**Chronostratigraphic distribution.** The oldest occurrence of this species is in the Bajocian, Middle Jurassic (Tiss et al., 2019) and it is extended until the and Berriasian (Martín-Closas, 2000). Its association with *Clavator grovesii* var. *jiuquanensis* (Fig. 2; Appendix 2) may indicate that this species has a very long timespan.

Family Clavatoraceae Pia, 1927

Subfamily Atopocharoidae (Grambast, 1968) emend. Martín-Closas ex Schudack, 1993

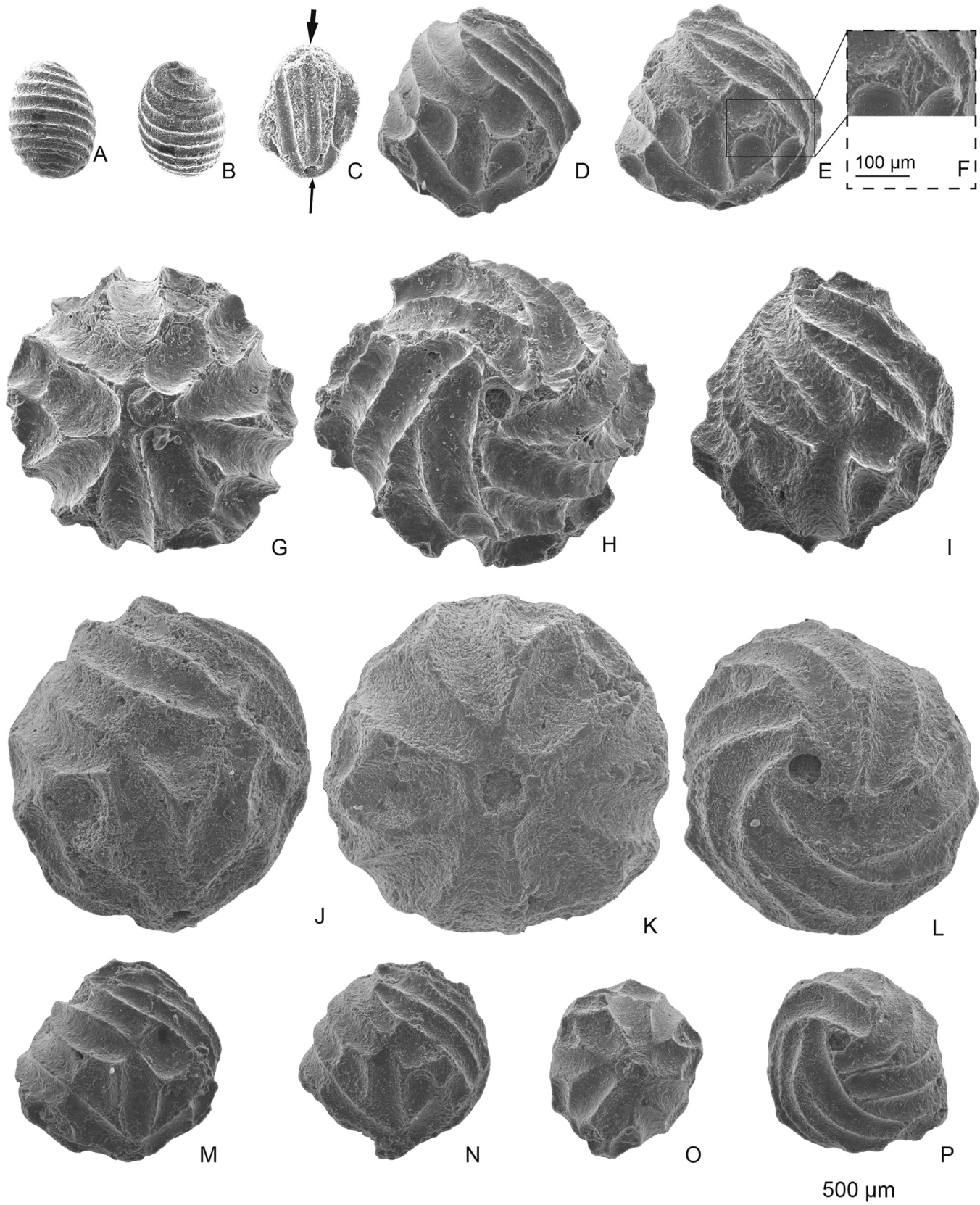


**Fig. 3.** SEM pictures of charophytes from the Arrifes section: *Porochara*, *Echinochara*, and *Atopochara*. A–B) *Porochara* cf. *fusca* (sample C127W; specimen Arr-Ch-1). A) Lateral view. B) Oblique-apical view, showing the apical pore. C) *Echinochara lazarii* (sample C152; specimen Arr-Ch-2). Wide arrow marks the apical neck of the gyrogonite. Thin arrow marks the basal rounded cell of the trifurcation. D–H) *Atopochara trivolis* var. *triquetra* (sample C127W). D–E) Lateral view (specimens Arr-Ch-3 and Arr-Ch-4); F) Antheridium shield; G) Basal view (specimen Arr-Ch-5); H) Apical view (specimen Arr-Ch-6). I–P) *Atopochara trivolis* var. *trivolis*. I) Lateral view (sample C127W; specimen Arr-Ch-7). J–P) *Atopochara trivolis* var. *trivolis* (sample C178). J–L) Bigger specimens. J) Lateral view (specimen Arr-Ch-8); K) Basal view (specimen Arr-Ch-9); L) Apical view (specimen Arr-Ch-10). M–P) Smaller specimens. M–N) Lateral view (specimens Arr-Ch-11 and Arr-Ch-12); O) Basal view (specimen Arr-Ch-13); P) Apical view (specimen Arr-Ch-14).

Genus *Echinochara* (Peck, 1957) emend. Pérez-Cano, Bover-Arnal et Martín-Closas, 2020

*Echinochara lazarii* (Martín-Closas, 2000) Mojon ex Pérez-Cano, Bover-Arnal et Martín-Closas, 2020

Fig. 3C

2000 *Echinochara peckii* var. *lazarii* nov. var. — Martín-Closas, p. 70, Pl. 6: figs. 1–8, Pl. 7: figs. 1–6.

2020 *Echinochara lazarii* (Martín-Closas, 2000) comb. nov. Mojon ex Pérez-Cano, Bover-Arnal et Martín-Closas — Pérez-Cano et al. p. 6–8, figs. 6–9.

**Description.** A few utricles of this species are only found in sample C152 (Appendix 2). This utricle is composed of two superimposed series of bract-cells that cover the gyrogonite in its abaxial part (see Pérez-Cano et al., 2020). However, all the specimens of this taxon found in the Arrifes section only preserve the inner series of the utricle, which is composed of the characteristic fork-like unit formed of three long cells basally attached to a small and rounded cell. Sometimes the cast of the non-calcified gyrogonite is found attached. This species is widely distributed in the Western Tethyan basins (Pérez-Cano et al., 2020 and references therein), but this is the first time that it is described in Portugal.

**Chronostratigraphic distribution.** This species is described between the lower Barremian and lower Aptian (Martín-Closas, 2009; Pérez-Cano et al., 2022a).

Genus *Atopochara* (Peck, 1938)

*Atopochara trivolvris* (Peck, 1938) emend. Martín-Closas, 1996

*Atopochara trivolvris* var. *triquetra* (Grambast, 1968) Martín-Closas, 1996

Fig. 3D–H

1968 *Atopochara trivolvris* subsp. *triquetra* subsp. nov. — Grambast, p. 9, Pl. 3, figs. 14A–C.

1996 *Atopochara trivolvris* var. *triquetra* (Grambast, 1968) Martín-Closas nov. comb. — Martín-Closas, p. 272, Figs. 8.

**Description.** Few utricles of this variety only appear in samples C32, C127E, and C127W (Appendix 2). In samples C127W and C127E, this variety is associated with *Atopochara trivolvris* var. *trivolvris*, being the latter dominant in the *Atopochara trivolvris* population (Appendix 2). Studied specimens correspond to the advanced morphotype defined by Martín-Closas and Grambast-Fessard (1986) and are distinguished by the observation of a very small antheridium shield imprint (Fig. 3F).

**Chronostratigraphic distribution.** This species firstly appears in the Hauterivian, where it is found associated with *Atopochara trivolvris* var. *ancora* (Grambast, 1967) Martín-Closas, 1996 (e.g., Martín-Closas and Salas, 1994). Homogeneous populations are firstly found at the base of the Barremian (Martín-Closas and Salas, 1994; Pérez-Cano et al., 2022a). In the upper Barremian–lower Aptian it is found associated with *Atopochara trivolvris* var. *trivolvris* Peck, 1938 (see Pérez-Cano et al., 2020, 2022a).

*Atopochara trivolvris* var. *trivolvris* Peck, 1938

Fig. 4I–P

1938 *Atopochara trivolvris* n. sp. — Peck, p. 173–176, Fig. 1; Pl. 28, figs. 5–12.

1996 *Atopochara trivolvris* var. *trivolvris* — Martín-Closas, p. 113–116, Pl. 9, figs. 9–10.

**Description.** These utricles are especially abundant in sample C178, where it forms homogeneous assemblages with bimodal distribution (Fig. 3J–L and M–P, respectively), but it is also dominant in samples C127E and C127W associated with *A. trivolvris* var. *triquetra*

(Appendix 2). This variety is distinguished from the previous one by having a more packed structure, more spiralized long cells, and very small to absence of the imprint of the antheridium shields.

**Chronostratigraphic distribution.** The older occurrence of this variety is in the upper Barremian, where few utricles of this species are found in a population dominated by *Atopochara trivolvris* var. *triquetra* (Pérez-Cano et al., 2020, 2022a). Homogeneous populations of this variety are found between the lower Aptian and the middle Albian (e.g., Martín-Closas, 2000; Álvarez-Parra et al., 2021).

Subfamily Clavatoroidae (Grambast, 1969) emend. Martín-Closas ex Schudack, 1993

Genus *Clavator* (Reid and Groves, 1916) emend. Martín-Closas ex Schudack, 1993

*Clavator grovesii* Harris, 1939

*Clavator grovesii* var. *jiuquanensis* (Wang, 1965) Grambast, 1970 emend. Martín-Closas, 1996

Fig. 4A–F

1965 *Perimneste jiuquanensis* sp. nov. — S.Wang, p. 467, Pl. 1.

1970 *Clypeator jiuquanensis* (S. Wang 1965) nov. comb. — Grambast, p. 1965, Fig. D; Pl. 3, figs. 1–5.

1973 *Clypeator europaeus* n. sp. — Mädlar in Neagu and Georgescu-Donos, p. 178, Pl. I, fig. 7–8; Pl. II, figs. 1–9.

1980a *Clypeator europaeus* Mädlar — Grambast-Fessard, p. 37–38, Fig. 1–2; Pl. 1, figs. 1–9; Pl. 3, fig. 2.

1996 *Clavator grovesii* var. *jiuquanensis* (Wang, 1965) Grambast, 1970 emend. — Martín-Closas, p. 278, Figs. 12.

**Description.** This species is common in the lower part of the stratigraphic section, being very abundant in samples C127E and C127W (Appendix 2). It is characterized by having a bilateral symmetry with two lateral and prominent cells-shields in which the 12 cells have the same length. Some specimens can have slightly twisted cells in the lateral shields with 13 cells (Fig. 4B–D). They are considered as intermediated morphologies between *C. grovesii* var. *jiuquanensis* and the *C. grovesii* var. *corrugatus*, i.e., *C. grovesii* var. *jiuquanensis* advanced or *C. grovesii* var. *corrugatus* primitive.

**Chronostratigraphic distribution.** This variety appears in the lower upper Barremian (Pérez-Cano et al., 2022a) and it is found in the upper Barremian and Aptian in the whole Eurasia (e.g., Martín-Closas, 2015; Li et al., 2020).

*Clavator grovesii* var. *corrugatus* (Peck, 1941) Martín-Closas, 1996 Fig. 4G–L

1941 *Perimneste corrugata* n. sp. — Peck, p. 295–297, Pl. 42, figs 15–24.

1962 *Clypeator corrugatus* (Peck, 1941) nov. comb. — Grambast, p. 295.

1980a *Clypeator lusitanicus* n. sp. — Grambast-Fessard, p. 39–41, Fig. 3; Pl. 1, fig. 10–12; Pl. 2, figs. 1–5; Pl. 3, fig 3–5.

1996 *Clavator grovesii* var. *lusitanicus* (Grambast-Fessard, 1980a) comb. nov. — Martín-Closas, p. 278, fig. 11.

1996 *Clavator grovesii* var. *corrugatus* (Peck, 1941) nov. comb. — Martín-Closas, p. 278, fig. 11.

2000 *Clavator grovesii* var. *corrugatus* (Peck, 1941) Martín-Closas, 1996 — p. 142–145, Pl. 14, figs. 10–12.

**Description.** The utricle of this species shows the characteristic bilateral symmetry, with two lateral bract-cell shields that are characterized by having 14 twisted cells. It first appears in samples C127E and C127W, where it represents <10% of the total population which is dominated by *Clavator grovesii* var. *jiuquanensis* (Appendix 2). *C. grovesii* var. *corrugatus* forms homogeneous populations in sample C178 upwards.



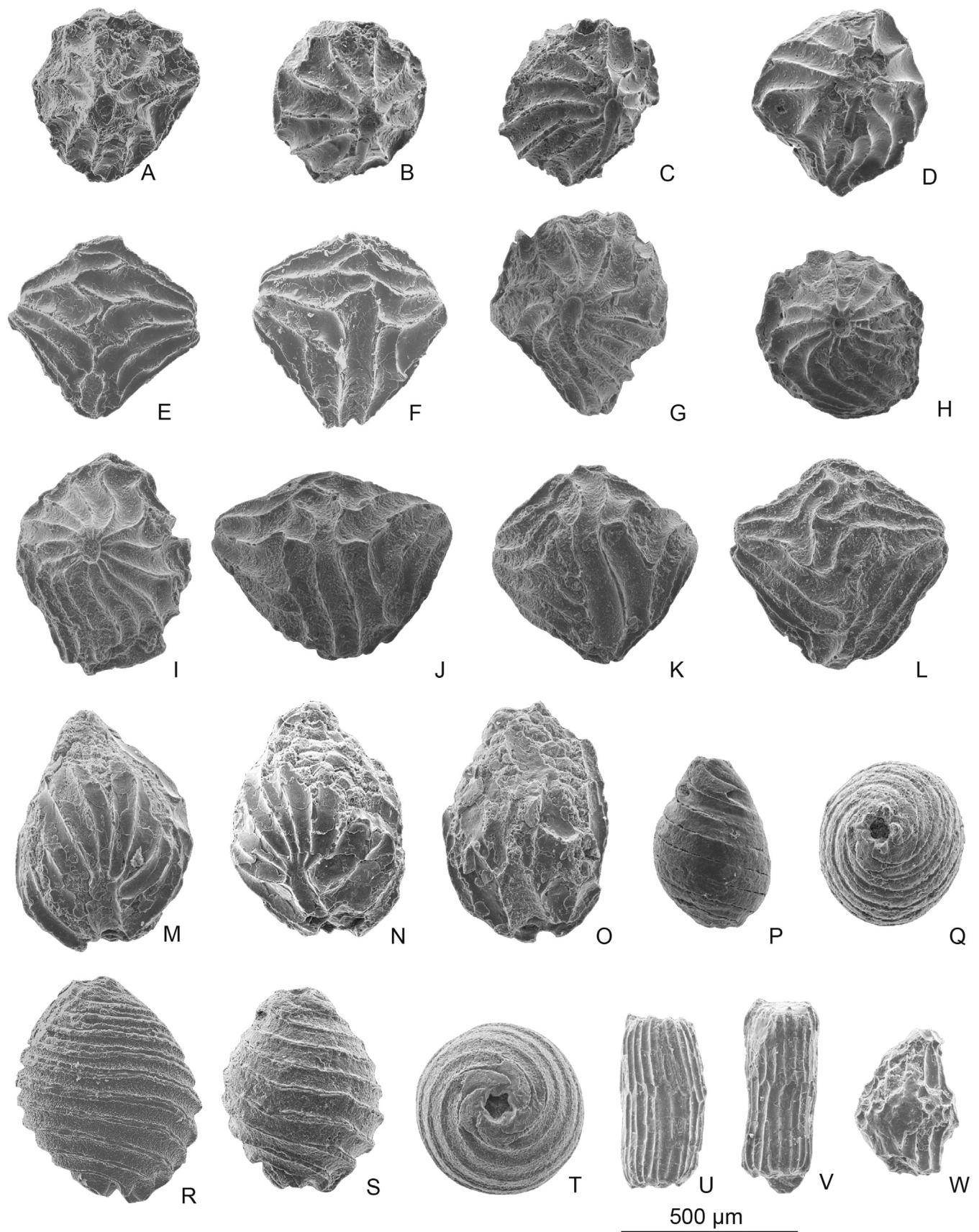


**Fig. 4.** SEM pictures of charophytes from the Arrifes section: utricles of genus *Clavator* and thalli portions. A–F) *Clavator grovesii* var. *jiuquanensis*. I) Lateral view of the typical morphotype (sample C127W; specimen Arr-Ch-15). B–D) Lateral views of the intermediate morphotype between *C. grovesii* var. *jiuquanensis* and *C. grovesii* var. *corrugatus*,



In the Algarve Basin, this species was described as *Clypeator lusitanicus* by Grambast-Fessard (1980a). Later, Soulié-Märsche (1994) compared the type population of *Clypeator corrugatus* with *Clypeator lusitanicus*, and observed that the morphology between both taxa was very similar. Following the strong similarities between both taxa, they were synonymized by Martín-Closas (2000).

**Chronostratigraphic distribution.** This taxon is found between the Aptian and lower-middle Albian in Europe of Western Europe and United States (Martín-Closas, 2000, 2015 and references therein).

*Clavator harrisii* (Peck, 1941) emend. Martín-Closas, 1996

*Clavator harrisii* var. *harrisii* Peck, 1941

Fig. 4M–O

1941 *Clavator harrisii* nov. sp. – Peck, p. 292–294, Pl. 42, figs. 25–37.  
1996 *Clavator harrisii* var. *harrisii* Peck – Martín-Closas, p. 278–279.

**Description.** Small populations of this species are found in samples C32, C127W, C127E, and C178. The utricles show the characteristic bilateral symmetry with two fans of cells in a lateral position. The posterior part shows strong similarities with the Barremian specimens described in Pérez-Cano (2021). It is always associated with *C. harrisii* var. *reyi* and *C. harrisii* var. *zavialensis*, being the latter taxa the dominant variety of the *C. harrisii* populations (Appendix 2).

**Chronostratigraphic distribution.** The chronostratigraphic distribution of this taxon is lower Valanginian–middle Albian. In the lower Valanginian, it appears associated with the older variety, *Clavator harrisii* var. *dongjingensis* (Hu and Zeng, 1981) Martín-Closas, 2000. *Clavator harrisii* var. *harrisii* usually forms homogeneous assemblages in the lower Barremian (Martín-Closas, 2000; Pérez-Cano et al., 2020, 2022a) but sometimes also in the Aptian (De Sosa Tomás et al., 2017) and in the lower-middle Albian (Álvarez-Parra et al., 2021). However, in the upper Barremian–lower Aptian it is frequently found associated with *Clavator harrisii* var. *reyi* (e.g., Martín-Closas, 2000; Pérez-Cano et al., 2020, 2022a), while in the upper Aptian to lower-middle Albian it is usually found forming mixed populations with *Clavator harrisii* var. *zavialensis* (e.g., Martín-Closas, 2000; Tibert et al., 2013; De Sosa Tomás et al., 2017).

*Clavator harrisii* var. *reyi* (Grambast-Fessard, 1980a) Martín-Closas, 1996

Fig. 4P–R

1980a *Stellatochara reyi* n. sp. – Grambast-Fessard, p. 42–44, Pl. 3, figs. 6–9.

1996 *Clavator harrisii* var. *reyi* (Grambast-Fessard, 1980a) nov. comb. – Martín-Closas p. 279.

2005 *Luzochara reyi* (Grambast-Fessard 1980a) nov. comb. – Pereira and Cabral, p. 173–178, Pl. 1, figs. 1–6.

**Description.** This species is found in samples C32, C127E, C127W, and C178. The specimens are characterized by only the gyrogonite with the convex cells separated by slightly undulated structures. In samples C127W and C178, there are observed gyrogonites whose cells show different degrees of calcification, showing convex and concave cells in the same gyrogonite (see Fig. 4R). These gyrogonites are considered as intermediate morphotypes between *C. harrisii* var.

*reyi* and *C. harrisii* var. *zavialensis* and they are referred them as *Clavator harrisii* var. *reyi* advanced or *Clavator harrisii* var. *zavialensis* primitive.

**Chronostratigraphic distribution.** The first occurrences of this taxon are in the lower Barremian, where it rarely appears associated to *C. harrisii* var. *harrisii*, which is the dominant variety (Pérez-Cano et al., 2020, 2022a). *Clavator harrisii* var. *reyi* is especially abundant and dominates the *Clavator harrisii* populations in the upper Barremian–lower Aptian where it forms homogeneous populations (e.g., Martín-Closas, 2000; Pereira and Cabral, 2005; Vicente and Martín-Closas, 2013) or can be associated to *C. harrisii* var. *harrisii*, being *C. harrisii* var. *reyi* dominant upon *C. harrisii* var. *harrisii* (Pérez-Cano et al., 2020, 2022a).

*Clavator harrisii* var. *zavialensis* (Grambast-Fessard, 1980a) Martín-Closas, 1996

Fig. 4S–T

1980 *Stenochara zavialensis* n. sp. – Grambast-Fessard, p. 44, Pl. 3, figs. 10–13.

1996 *Clavator harrisii* var. *zavialensis* (Grambast Fessard, 1980a) nov. comb. – Martín-Closas, p. 279.

**Description.** *Clavator harrisii* var. *zavialensis* represents the last variety of the evolutionary lineage of *Clavator harrisii* (see Martín-Closas, 1996) and it is characterized by preserving only the gyrogonite that has slightly concave spiralled units separated by a double ridge. The Ringstruktur-calcification pattern, described by Schudack (1993) for clavatoroid gyrogonites is often visible at the apical tips of the spiral cells. In the Arrifes section, this taxon always appears associated to *C. harrisii* var. *reyi* and *C. harrisii* var. *harrisii*.

**Chronostratigraphic distribution.** This variety of *Clavator harrisii* is found in the upper Aptian–lower Albian, when it usually forms homogeneous assemblages (see e.g., Martín-Closas, 2000; Trabelsi et al., 2016).

#### 4.2. Charophyte thalli

Genus *Munieria* (Deecke, 1883) emend. Granier in Granier et al., 2015

*Munieria grambastii* Bystrický, 1976

Fig. 4U

1976 *Munieria grambastii* n. sp. – Bystrický, p. 48–54, Pl. I, figs. 1–14; Pl. II, figs. 1–16; Pl. IV, fig. 2.

2020 *Munieria grambastii* Bystrický 1976 – Pérez-Cano et al. p. 21–22, Firgghs. 16A–G, Fihug. 17A–K

**Description.** A few small portions of this thallus (isolated internodes) are found in samples C127E and C127W, C178, and C182. The biological affinity of *Munieria* has been extensively discussed, as it has been attributed to charophytes (e.g., Martín-Closas, 2000; Pérez-Cano et al., 2020) or dasylacadeans (Feist et al., 2003). The interdigitation of the cortical cells in the middle part of the internode and the inner growth of the internode (Martín-Closas, 2000; Pérez-Cano et al., 2020; respectively), demonstrated its pertaining

(*C. grovesii* var. *jiuquanensis* advanced or *C. grovesii* var. *corrugatus* primitive). B–C) (sample C127E; specimens Arr-Ch-16 and Arr-Ch-17); D) sample C127W; specimen Arr-Ch-18) E) Abaxial view (sample C127W; specimen Arr-Ch-19); F) Adaxial view (sample C127W; specimen Arr-Ch-20). G–L) *Clavator grovesii* var. *corrugatus* (sample C178). G–I) Lateral view, showing different morphologies of the shield (specimens Arr-Ch-21, Arr-Ch-22, and Arr-Ch-23). J–K) Adaxial view (specimens Arr-Ch-24 and Arr-Ch-25). L) Abaxial view (specimen Arr-Ch-26). M–O) *Clavator harrisii* var. *harrisii* (sample C127W). M–N) Lateral view. Each specimen shows different morphologies of the lateral fan (specimens Arr-Ch-27 and Arr-Ch-28). P) Adaxial view, showing the phylloid imprint and different cells at the top that completely cover the gyrogonite in the adaxial part (specimen Arr-Ch-29). P–Q) *Clavator harrisii* var. *reyi*. P) Lateral view (sample C32; specimen Arr-Ch-30); Q) Apical view (sample C178; specimen Arr-Ch-31). R) Lateral view of the morphotype between *C. harrisii* var. *reyi* and *C. harrisii* var. *zavialensis* (*C. harrisii* var. *reyi* advanced or *C. harrisii* var. *zavialensis* primitive), (sample C127W; specimen Arr-Ch-32). S–T) *Clavator harrisii* var. *zavialensis*. S) Lateral view (sample C178; specimen Arr-Ch-33). T) Apical view (sample C127W; specimen Arr-Ch-34). U–V) Charophyte thalli. U–V) *Munieria grambastii* (sample C127W, specimens Arr-Ch-35 and Arr-Ch-36, respectively). W) *Clavatoraxis* sp. (sample C127W, specimen Arr-Ch-37).

to the Clavatoraceae family. This thallus morphology is associated with some species of the genus *Clavator* except *Clavator harrisii*.

Genus *Clavatoraxis* Martín-Closas et Diéguez, 1998

***Clavatoraxis* sp.**

**Fig. 4V**

**Description.** This thallus morphology has been found in samples C127W, and C178. It consists of a corticated thallus with the characteristic hemispherical spine-cell rosettes upon the cortical cells. The portions are very short, impeding their identification at the specific level. This thallus morphology has been associated to the species *Atopochara trivolis* (e.g., Martín-Closas, 2000) and *Clavator harrisii*, the latter due to the anatomical connection between both organs (e.g., De Sosa Tomás et al., 2017; Pérez-Cano, 2021).

## 5. Charophyte biostratigraphy and correlation with marine domain

The present work follows the charophyte biozonation proposed by Riveline et al. (1996) and later modified by Martín-Closas et al. (2009) and Pérez-Cano et al. (2022a). These biozones are partial range biozones, i.e., defined by the FAD of index species (or at the first homogeneous population in the case of the anagenetic lineages), but with the inclusion of several other species that enabled to identify of the biozone in the case that the index species is not observed. By the way, these biozones can be considered equivalent to assemblage biozones or Oppelzones. Two clavatoracean assemblages with biostratigraphic interest are distinguished in the middle to upper part of the studied Arrifes section and are correlated with the dinoflagellate cyst biozones previously described in the section (Fig. 2).

### 5.1. Upper Barremian–lower Aptian

The lower assemblage is described between 65 m and 135 m of the stratigraphic section (Fig. 2), and it is characterized by the association of *Echinochara lazarii*, mixed populations of *Atopochara trivolis* var. *triquetra* and *Atopochara trivolis* var. *trivolis*, mixed populations of *Clavator grovesii* var. *jiuquanensis* and *Clavator grovesii* var. *corrugatus* (rare) and intermediate morphotypes between both taxa, and mixed populations of *Clavator harrisii* var. *harrisii*, *Clavator harrisii* var. *reyi*, and *Clavator harrisii* var. *zavialensis*, and intermediate morphotypes between *C. harrisii* var. *reyi* and *C. harrisii* var. *zavialensis*. Based on the occurrence of *Clavator grovesii* var. *jiuquanensis*, this charophyte association has been ascribed to the upper Barremian–lower Aptian *Clavator grovesii* var. *jiuquanensis* Eurasian biozone (Pérez-Cano et al., 2022a). This charophyte assemblage partially corresponds to the upper lower Barremian–lower Aptian *Asci-diella cruciata*-*Pseudoglobator paucibracteatus* European biozone (see, Pérez-Cano et al., 2022a).

The lowermost part of the upper Barremian–lower Aptian *Clavator grovesii* var. *jiuquanensis* biozone could be correlated with the occurrence of *Subtilisphaera scabrata* dinoflagellate cyst biozone (Fig. 2; Mendes et al., 2023). This key dinoflagellate cyst ranges from the FO of the aforementioned species to the FO of *Odontochitina operculata* (Leereveld, 1995, 1997), being assigned to the lower Barremian–lowermost upper Barremian. The upper part of the *Clavator grovesii* var. *jiuquanensis* biozone is correlated with the *Odontochitina operculata* dinoflagellate cyst biozone (Fig. 2). The *Clavator grovesii* var. *jiuquanensis* biozone was tentatively correlated with the key marine dinoflagellate cyst identified by Mendes et al. (2023) for the Arrifes section.

The correlation between the *Clavator grovesii* var. *jiuquanensis* biozone with the dinoflagellate biozones is in agreement with the previous correlation of both biozones with the ammonite biozonation. Thus, the base of *C. grovesii* var. *jiuquanensis* biozone was correlated with the *Toxancyloceras vandenheckii* ammonite biozone, based on a direct correlation between both biozones (Martín-Closas et al., 2009) and Sr-isotope stratigraphy (Pérez-Cano et al., 2022a). The upper part of the *Subtilisphaera scabrata* biozone was also correlated with the *T. vandenheckii* ammonite biozone (Leereveld, 1995, 1997). Moreover, charophyte assemblages that belong to the European *Asci-diella cruciata*-*Pseudoglobator paucibracteatus* charophyte biozone and the Eurasian *Clavator grovesii* var. *jiuquanensis* charophyte biozone were correlated against the lower Aptian *Deshayesites weisii* ammonite biozone (*Deshayesites forbesi* ammonite biozone according to Reboulet et al., 2011) in the Subalpine Chains and Jura Mountains (Martín-Closas et al., 2009; Fig. 5). Furthermore, *Clavator grovesii* var. *jiuquanensis* is also described in lower Aptian strata that were chemostratigraphically correlated with the marine domain in the Chinese basins (Li et al., 2020). *Odontochitina operculata* biozone is also correlated with the lower Aptian ammonite biozones (Leereveld, 1995, 1997).

### 5.2. Lower Aptian

The second assemblage is described from the 135 m until the top of the section (Fig. 2) and is characterized by the co-occurrence of homogeneous populations of *Atopochara trivolis* var. *trivolis*, homogeneous populations of *Clavator grovesii* var. *corrugatus*, *Clavator harrisii* var. *harrisii*, *Clavator harrisii* var. *reyi*, and *Clavator harrisii* var. *zavialensis*. This assemblage corresponds to the typical assemblage of the *Clavator grovesii* var. *lusitanicus* biozone of Riveline et al. (1996), which was described on the basis of the Tincup Creek biozone of Grambast (1974). The First Occurrence (FO) of *C. grovesii* var. *corrugatus* in the Arrifes section is in a sample in which it is associated with *C. grovesii* var. *jiuquanensis* (C127W; Fig. 2). However, in the case of anagenetic lineages the occurrence of mixed populations with two varieties that also contain specimens that are intermediate morphotypes between two varieties is very common (e.g., Martín-Closas, 1989; Martín-Closas and Salas, 1994; Pérez-Cano et al., 2020, 2022a). For this reason, in the present work, the base of the biozone is pointed at the first homogeneous population of *C. grovesii* var. *corrugatus* (Fig. 2), at sample C178, following the criterion established in Pérez-Cano et al. (2022a) for biozones based on anagenetic varieties.

*Clavator grovesii* var. *lusitanicus* was synonymized to *Clavator grovesii* var. *corrugatus* by Martín-Closas (2000). Following this synonymy, the charophyte biozone *Clavator grovesii* var. *lusitanicus* of Riveline et al. (1996) is here redefined as follows:

Name: *Clavator grovesii* var. *corrugatus*.

Definition: Partial range biozone defined between the FAD of homogeneous populations of *Clavator grovesii* var. *corrugatus* and homogeneous populations of *Atopochara trivolis* var. *restric-ta* (Grambast-Fessard 1980b) Martín-Closas 1996.

Correlations: In the Arrifes section, the base of *Clavator grovesii* var. *corrugatus* biozone is placed in a marly layer inside an interval that contains the dinoflagellate key taxa *Odontochitina operculata* and attributed to the homonymous biozone (Fig. 2; Mendes et al., 2023). This interval is defined by the occurrence of this taxon, and ranges from the FO of *Odontochitina operculata* to the FO of *Cribroperidinium tenuiceras*, indicating an age no older than the late Barremian (Costa and Davey, 1992; Leereveld, 1995, 1997). The base and the top of this dinoflagellate biozone are also well-correlated with the standard ammonite biozonations. Thus, the FO of *O. operculata* is correlated with the *Toxancyloceras vandenheckii*

		Standard Ammonite biozones	Dinoflagellate biozones	Charophyte biozones	
				European	Eurasian
Aptian	upper	<i>Hypacanthoplites jacobi</i>	<i>Cribopteridinium tenuiceras</i>	<i>Clavator grovesii</i> var. <i>corrugatus</i>	
		<i>Acanthohoplites nolani</i>			
		<i>Parahoplites melchioris</i>			
		<i>Epicheloniceras martini</i>			
	lower	<i>Dufrenoyia furcata</i>	<i>Odontochitina operculata</i>		
		<i>Deshayesites deshayesi</i>			
		<i>Deshayesites forbesi</i>		<i>Asciidiella cruciata</i> - <i>Pseudoglobator paucibracteatus</i>	<i>Clavator grovesii</i> var. <i>jiuquanensis</i>
		<i>Deshayesites ogilensis</i>			
Barremian	upper	<i>Martelites sarasini</i>	<i>Subtilisphaera scabrata</i>		
		<i>Imerites giraudi</i>			
		<i>Gerhardtia sartousiana</i>			
		<i>Toxancyloceras vandenheckii</i>			

**Fig. 5.** Correlation of the upper Barremian–lower Aptian charophyte biozones with the dinoflagellates biozones and the standard ammonite biostratigraphy. Ammonite biozonation after the latest proposal of [Reboullet et al. \(2018\)](#). Dinoflagellate biozonation after [Leereveld \(1995, 1997\)](#) and [Moullade et al. \(1998\)](#). Dinoflagellate biozonation includes those biozones identified in the studied section, i.e., *Subtilisphaera scabrata* and *Odontochitina operculata* (see [Mendes et al., 2023](#)), and follows the biozonation schemes proposed by [Leereveld \(1995, 1997\)](#). Charophyte biozonation partially modifies the proposal of [Pérez-Cano et al. \(2022a\)](#). Greyish Area corresponds to the range in which the base of *C. grovesii* var. *corrugatus* biozone must be placed (see explanation in text). The comparison with other charophyte biozonations can be seen in [Appendix 3](#).

ammonite biozone ([Leereveld, 1995, 1997](#)), while the FO of *Cribroperidinium tenuiceras* correlates with the *Dufrenoyia furcata* ammonite biozone ([Moullade et al., 1998](#)) close to the lower–upper Aptian boundary ([Masure et al., 1998](#)). The FO of *C. tenuiceras* was used as a tentative marker for the lower–upper Aptian boundary in the Luz section, in the western part of the Algarve Basin ([Heimhofer et al., 2007](#)). However, this key taxon was not recorded in the Arrifes section ([Mendes et al., 2023](#)).

The base of the *Clavator grovesii* var. *lusitanicus* biozone of [Riveline et al. \(1996\)](#) was placed in the lower–upper Aptian boundary. However, only the upper part of this biozone (lower Albian) was previously correlated with the coeval marine biostratigraphy ([Riveline et al., 1996](#) and references therein). The direct correlation between the FAD of the first homogeneous population of *C. grovesii* var. *corrugatus*, considered the base of the *Clavator grovesii* var. *corrugatus* biozone, and the *O. operculata* dinoflagellate

biozone indicates that the base of the *Clavator grovesii* var. *corrugatus* biozone must be lower Aptian, below the lower–upper Aptian boundary.

Following previous correlations of the *Clavator grovesii* var. *jiuquanensis* biozone against the standard ammonite biostratigraphy (see chapter 5.1), and the direct correlation of the base *Clavator grovesii* var. *corrugatus* biozone with the *Odontochitina operculata* dinoflagellate biozone described in this work, the base of the *Clavator grovesii* var. *corrugatus* biozone must be upper lower Aptian, between the top of the *Deshayesites forbesi* and the *Dufrenoyia furcata* ammonite biozones ([Fig. 5](#)). The top of this charophyte biozone is in the middle Albian, as charophyte assemblages of this biozone are correlated against middle Albian ammonite biozones (see [Riveline et al., 1996](#) and references therein).

Horizon: upper lower Aptian–middle Albian.



## 6. Conclusions

The present study shows a marine-continental correlation between the charophyte biozones and the dinoflagellate key taxa previously described in the Arrifes section (Algarve Basin, Portugal) in the upper Barremian–Aptian record. This is the first time that these two biochronologies can be directly correlated and it has allowed the improvement of the charophyte biochronology and biostratigraphy of the Aptian record.

The *Clavator grovesii* var. *jiuquanensis* biozone is identified by the occurrence of the index species, *Clavator grovesii* var. *jiuquanensis*, and the clavatoracean species associated, including *Echinochara lazarii*, *Atopochara trivolvii* var. *triquetra* and *A. trivolvii* var. *trivolvii*, *Clavator harrisii* var. *harrisii*, *Clavator harrisii* var. *reyi*, and *C. harrisii* var. *zavialensis*. The base of this biozone at the Arrifes section is directly correlated with the occurrence of the dinoflagellate cyst *Subtilisphaera scabrata*. This correlation agrees with previous correlations with the *Toxanclyoceras vandenheckii* ammonite biozone made for each biozone and reinforces the previous timespan suggested for this biozone.

The *C. grovesii* var. *corrugatus* biozone is described after the occurrence of the index species, *C. grovesii* var. *corrugatus*, that is associated with *A. trivolvii* var. *trivolvii*, *Clavator harrisii* var. *harrisii*, *Clavator harrisii* var. *reyi*, and *Clavator harrisii* var. *zavialensis*. The base of this biozone is correlated with the occurrence of the dinoflagellate cyst *Odontochitina operculata*, as well as, with the standard ammonite biozonation. This enables to redefine of the lower boundary of the *C. grovesii* var. *corrugatus* biozone to the upper lower Aptian, between the *Deshayesites forbesi* and the *Dufrenoyia furcata* ammonite biozones. Consequently, the total timespan of *C. grovesii* var. *corrugatus* biozone is upper lower Aptian–middle Albian. The use of chemostratigraphic methods should help to pinpoint with more precision the base of the *C. grovesii* var. *corrugatus* biozone in the upper lower Aptian, inside the interval defined by the previously mentioned ammonite biozones.

These two charophyte biozones (i.e., *Clavator grovesii* var. *jiuquanensis* and *Clavator grovesii* var. *corrugatus*) are described in the Arrifes section. These charophyte biozone contains intermediate morphotypes between *Clavator grovesii* var. *jiuquanensis* and *C. grovesii* var. *corrugatus* and intermediate morphotypes between *Clavator harrisii* var. *reyi* and *C. harrisii* var. *zavialensis*, indicating sedimentary continuity along the upper part of the section. These features highlight the unique palaeobotanical and biostratigraphical context of the Algarve Basin, featuring the importance of the Arrifes section as an excellent candidate to become the type section for the Aptian charophyte biostratigraphy.

## Data availability

Data will be made available on request.

## Acknowledgements

This study was partially funded by and is a contribution to the project IBERINSULA (PID2020-113912GB-I00), funded by MCIN/AEI/10.13039/501100011033 and the European Regional Development Fund (ERDF). This study also had the financial support Fundação para a Ciência e Tecnologia (FCT), under the projects UIDB/00611/2020 and UIDP/00611/2020 CITEUC and LA/P/0069/2020 granted to the Associate Laboratory ARNET and UID/00350/2020 CIMA. JP-C Margarita Salas postdoctoral contract and research is supported by the Ministerio de Universidades of Spain, “Plan de recuperación, transformación y resiliencia” of Spanish Government and the Next Generation funds from the European Union. Dr.

Alejandro Gallardo (technician of the Palaeontological Laboratory of the Departament de Dinàmica de la Terra i de l’Oceà) is acknowledged for his assistance in preparing the samples studied here. The manuscript has been highly improved during the peer-review after the detailed revisions and suggestions of the editor, Dr. Eduardo Koutsoukos, and the reviewers, Dr. Carles Martín-Closas (University of Barcelona), Dr. Alba Vicente (Instituto Politécnico Nacional, La Paz, México), and Dr. Khaled Trabelsi (University of Vienna). Dr. Carles Martín-Closas is also acknowledged for the productive discussions in the early stages of this work.

## References

- Álvarez-Parra, S., Pérez-de la Fuente, R., Peñalver, E., Barrón, E., Alcalá, L., Pérez-Cano, J., Martín-Closas, C., Trabelsi, K., Meléndez, N., López Del Valle, R., Lozano, R.P., Peris, D., Rodrigo, A., Sarto i Montey, V., Bueno-Cebollada, C.A., Menor-Salván, C., Philippe, M., Sánchez-García, A., Peña-Kairath, C., Arillo, A., Espílez, E., Mampel, L., Delclós, X., 2021. Dinosaur bonebed amber from an original swamp forest soil. *eLife* 10, e72477.
- Azeredo, A., Duarte, L., Henriques, M., Manuppella, G., 2003. Da dinâmica continental no Triásico aos mares do Jurássico Inferior e Médio. *Cadernos de Geologia de Portugal*. Instituto Geológico e Mineiro, Lisboa, 43 pp.
- Berthou, P.Y., Leereveld, H., 1990. Stratigraphic implications of palynological studies on Berriasian to Albian deposits from western and southern Portugal. *Review of Palaeobotany and Palynology* 66, 313–344.
- Berthou, P.Y., Correia, F., Prates, S., Taugourdeau, J., 1983. Essai de synthèse du Crétacé de l’Algarve: biostratigraphie, paléogéographie et sédimentation argileuse. I: biostratigraphie et paléogéographie. *Bulletin d’Information des Géologues du Bassin de Paris* 20 (2), 3–18.
- Borges, M., Riding, J., Fernandes, P., Pereira, Z., 2011. The Jurassic (Pliensbachian to Kimmeridgian) palynology of the Algarve Basin and the Carrapateira outlier, southern Portugal. *Review of Palaeobotany and Palynology* 163, 190–204.
- Borges, M., Riding, J., Fernandes, P., Matos, V., Pereira, Z., 2012. Callovian (Middle Jurassic) dinoflagellate cysts from the Algarve Basin, southern Portugal. *Review of Palaeobotany and Palynology* 170, 40–56.
- Bover-Arnal, T., Moreno-Bedmar, J.A., Frijia, G., Pascual-Cebrian, E., Salas, R., 2016. Chronostratigraphy of the Barremian–early Albian of the Maestrat Basin (E Iberian Peninsula): integrating strontium-isotope stratigraphy and ammonoid biostratigraphy. *Newsletters on Stratigraphy* 49 (1), 41–68.
- Bystrický, J., 1976. *Munieria grambasti* sp. nov. in Kalk Gerölle des Uplav-Konglomerate des Mittleren Váh-Gebietes (Klippenzone, Westkarpaten). *Geologica Carpathica* 27 (1), 45–64.
- Correia, F.M.C., 1989. Estudo biostratigráfico e microfácies do Cretácico carbonatado da bacia sedimentar meridional Portuguesa (Algarve). University of Lisbon, Lisbon, 377 pp.
- Costa, L.I., Davey, R.J., 1992. Dinoflagellate cysts of the Cretaceous System. In: Powell, A.J. (Ed.), *A Stratigraphic Index of Dinoflagellate Cysts*. Chapman & Hall, London, pp. 99–154.
- De Sosa Tomás, A., Vallati, P., Martín-Closas, C., 2017. Biostratigraphy and biogeography of charophytes from the Cerro Barcino Formation (upper Aptian–Lower Albian), Cañadón Asfalto Basin, central Patagonia, Argentina. *Cretaceous Research* 79, 1–11.
- Deecke, W., 1883. Über einige neue Siphonien. *Neues Jahrbuch für Mineralogie. Geologie und Paläontologie* 1, 1–14.
- Dommergues, J.L., Meister, C., Rocha, R., 2011. The Pliensbachian ammonites of the Algarve Basin (Portugal) and their palaeobiogeographical significance for the “Iberia-Newfoundland” conjugate margins. *Swiss Journal of Geosciences* 104, 81–96.
- Feist, M., Wang, Z., 1995. The species concept in Clavatoraceae (fossil Charophyta) reviewed. *Taxon* 44, 351–361.
- Feist, M., Génot, P., Grambast-Fessard, N., 2003. Ancient Dasycladales and Charophyta convergences and differences with special attention to *Munieria baconica*. *Phycologia* 42 (2), 123–132.
- Fernandes, P., Rodrigues, B., Borges, M., Matos, V., Clayton, G., 2013. Organic maturation of the Algarve Basin (southern Portugal) and its bearing on thermal history and hydrocarbon exploration. *Marine and Petroleum Geology* 46, 210–233.
- Grambast, L., 1962. Classification de l’embranchement des charophytes. *Naturalia Monspeliensis, Série Botanique* 14, 63–86.
- Grambast, L., 1967. La série évolutive *Perimneste-Atopochara* (Charophytes). *Comptes rendus de l’Académie des Sciences* 264, 581–584.
- Grambast, L., 1968. Evolution of the utricle in the charophyta genera *Perimneste* Harris and *Atopochara* Peck. *Journal of the Linnean Society (Botany)* 61, 5–11.
- Grambast, L., 1969. La symétrie de l’utricle chez les Clavatoracées et sa signification phylogénétique. *Comptes rendus de l’Académie des Sciences* 269, 878–881.
- Grambast, L., 1970. Origine et évolution des *Clypeator* (Charophytes). *Comptes rendus de l’Académie des Sciences* 271, 1964–1967.
- Grambast, L., 1974. Phylogeny of the Charophyta. *Taxon* 23, 463–481.
- Grambast-Fessard, N., 1980a. Quelques espèces de *Clypeator* Grambast (Clavatoraceae) et les charophytes associées du Crétacé inférieur du Portugal. *Revue de Micropaléontologie* 23, 37–47.

- Grambast-Fessard, N., 1980b. Description de deux espèces nouvelles d'*Atopochara* Peck (Clavatoraceae, Charophyta). *Geobios* 13 (1), 129–135.
- Grambast-Fessard, N., 1986. Deux nouveaux représentants du genre *Asciidiella* (Clavatoraceae, Charophyta). *Geobios* 19, 255–260.
- Granier, B., Azar, D., Maksoud, S., Gèze, R., Habchi, R., 2015. New fossiliferous sites with Barremian Charophyta in the “Grès du Liban auct. (Lebanon), with a critical perspective regarding the nature of *Munieria* Deecke, 1883. *Carnets de Géologie* 15 (15), 199–229.
- Hardenbol, J., Thierry, J., Farley, M.B., Jacquin, T., de Gracianski, P.C., Vail, P.R., 1998. Mesozoic and Cenozoic sequence chronostratigraphic framework of European basins. In: de Gracianski, P.C., Hardenbol, J., Jacquin, T., Vail, P.R. (Eds.), *Mesozoic and Cenozoic Sequence Stratigraphy of European Basins*, vol. 60. SEPM Special Publications, pp. 3–13.
- Harris, T.M., 1939. British Purbeck Charophyta. British Museum (Natural History), London, pp. 1–83.
- Heimhofer, U., Hochuli, P.A., Burla, S., Weissert, H., 2007. New records of Lower Cretaceous angiosperm pollen from Portuguese coastal deposits: Implications for the timing of the early angiosperm radiation. *Review of Palaeobotany and Palynology* 144, 37–76.
- Hochuli, P.A., Heimhofer, U., Weissert, H., 2006. Timing of early angiosperm radiation: recalibrating the classical succession. *Journal of the Geological Society* 163, 587–594.
- Hu, J., Zeng, D., 1981. Early Cretaceous Charophytes from Hengyang Basin, Hunan. First Convention of the Micropaleontological Society of China 1979. Science Press, Beijing, pp. 144–151 (in Chinese).
- Leereveld, H., 1995. Dinoflagellate cysts from the Lower Cretaceous Rio Argos succession (SE Spain). LPP Foundation, Utrecht, pp. 1–175.
- Leereveld, H., 1997. Hauterivian–Barremian (Lower Cretaceous) dinoflagellate cyst stratigraphy of the western Mediterranean. *Cretaceous Research* 18, 421–456.
- Li, S., Wang, Q., Zhang, H., 2020. Charophytes from the Lower Cretaceous Xiagou Formation in the Jiuquan Basin (northwestern China) and their palaeogeographical significance. *Cretaceous Research* 105, 103940.
- Lindley, J., 1836. A natural system of Botany. Longman, London, 526 pp.
- Mädler, K., 1952. Charophyten aus dem Nordwestdeutschen Kimmeridge. *Geologisches Jahrbuch* 67, 1–46.
- Mädler, K., 1955. Zur Taxonomie der Tertiären Charophyten. *Geologisches Jahrbuch* 70, 265–328.
- Manuppella, G., 1988. Litoestratigrafia e tectónica da Bacia Algarvia. *Geonovas* 10, 67–71.
- Manuppella, G., 1992. Carta Geológica da Região do Algarve na escala 1/100000. Geológicos de Portugal, Lisboa.
- Manuppella, G., Ramalho, M., Antunes, A., Pais, J., 1987. Carta Geológica de Portugal na escala 1:50 000, Notícia Explicativa da Folha 53-A (Faro). Serviços Geológicos de Portugal, Lisboa, 52 pp.
- Marques, B., Rocha, R., 1988a. O Caloviano do flanco norte do Guilhim (Algarve oriental): biostratigrafia e paleobiogeografia. *Ciencias da Terra* 9, 19–26.
- Marques, B., Rocha, R., 1988b. Evolução paleogeográfica e paleobiogeográfica do Caloviano-Kimmeridgiano do Algarve. *Ciencias da Terra* 9, 33–40.
- Martín-Closas, C., 1989. Els caròfits del Cretaci inferior de les conques perifèriques del Bloc de l'Ebre. PhD thesis. Universitat de Barcelona, Barcelona, 608 pp.
- Martín-Closas, C., 1996. A phylogenetic system of Clavatoraceae (Charophyta). *Review of Palaeobotany and Palynology* 94, 259–293.
- Martín-Closas, C., 2000. Els caròfits del Juràssic superior i Cretaci inferior de la Península Ibèrica. *Arxius de les Seccions de Ciències*, vol. 125. Institut d'Estudis Catalans, Barcelona, 304 pp.
- Martín-Closas, C., 2015. Cosmopolitanism in Northern Hemisphere Cretaceous Charophyta (Clavatoridae). *Palaeogeography, Palaeoclimatology, Palaeoecology* 438, 9–23.
- Martín-Closas, C., Diéguez, C., 1998. Charophytes from the Lower Cretaceous of the Iberian Ranges (Spain). *Palaeontology* 41, 1133–1152.
- Martín-Closas, C., Grambast-Fessard, N., 1986. Les charophytes du Crétacé inférieur de la région du Maestrat (Chaîne Ibérique, Catalanides, Espagne). *Paleobiologie Continentale* 15, 1–66.
- Martín-Closas, C., Salas, R., 1994. Lower Cretaceous Charophytes. Biostratigraphy and evolution in the Maestrat Basin (Eastern Iberian Ranges). In: VIII Meeting of the European group of Charophyte Specialists Fieldtrip Guidebook. Diagonal, Barcelona, p. 89.
- Martín-Closas, C., Schudack, M., 1997. On the concept of species in fossil Charophyta. A reply to Feist & Wang. *Taxon* 46, 521–525.
- Martín-Closas, C., Clavel, B., Charollais, J., Conrad, M.A., 2009. Charophytes from the Barremian-lower Aptian of the Northern Subalpine Chains and Jura Mountains, France: correlation with associated marine assemblages. *Cretaceous Research* 30, 49–62.
- Masure, E., Raynaud, J.F., Pons, D., de Reneville, P., 1998. Palynologie du stratotype historique de l'Aptien inférieur dans la région de Cassis-La Bédoule (SE France). *Geologie Méditerranéenne* 25 (3), 263–287.
- Mendes, M., Descamps, G.S., Fernandes, P., Lopes, G., Jorge, R.C.G.S., Pereira, Z., 2023. The upper Hauterivian–Barremian Lower Cretaceous Arrifes section (Algarve Basin, Southern Portugal): a palynostratigraphic and palaeoenvironmental approach. *Cretaceous Research* 144, 105433.
- Migula, W., 1897. Die Characeen Deutschlands. Österreichs und der Schweiz. In: Rabenhorst, X. (Ed.), *Kryptogamic Flora*, vol. 5. E. Kummer, Leipzig, 765 pp.
- Mojon, P.O., 1996. Précisions sur l'intervalle Valanginién–Barremien de la biozonation des Charophytes du Crétacé inférieur du Maestrat (Chaîne Ibérique Orientale, Espagne) et sur la biozonation des Charophytes de l'intervalle Jurassique supérieur–Crétacé de l'Europe occidentale. *Geologie Alpine* 72, 61–99.
- Mojon, P.O., 2002. Les formations mésozoïques à Charophytes (Jurassique moyen–Crétacé inférieur) de la marge téthysienne nor-occidentale (Sud-est de la France, Suisse occidentale, nord-est de l'Espagne). *Sédimentologie, micropaléontologie, biostratigraphie. Géologie Alpine*, vol. 41. Mémoires Hors Série, p. 386.
- Moullade, M., Masse, J.P., Tronchetti, G., Kuhnt, W., Ropolo, P., Berge, J.-A., Madure, E., Renard, M., 1998. Le stratotype historique de l'Aptien inférieur (région de Cassis-La Bédoule): synthèse stratigraphique. *Geologie Méditerranéenne* 25 (3), 289–298.
- Musacchio, E.A., 1989. Biostratigraphy of non-marine Cretaceous of Argentina based on Calcareous microfossils. In: Wiedman, J. (Ed.), *Cretaceous of the Western Tethys. Proceedings of the 3rd International Cretaceous Symposium*, Tübingen 1987. E. Schweizerbart'sche Verlagsbuchhandlung, Stuttgart, pp. 811–850.
- Musacchio, E.A., 2000. Biostratigraphy and biogeography of Cretaceous Charophytes from South America. *Cretaceous Research* 21, 211–220.
- Neagu, T., Georgescu-Donos, M.O., 1973. Characeae Eocretacice die Dobrogea de Sud (Valea Akargea-Pestera). Studii si cercetari de geologie, geofizice si geografie 18, 171–185 (in Romanian).
- Oliveira, J.T., Pereira, E., Ramalho, M., Antunes, M., Monteiro, J., 1992. Carta Geológica de Portugal. Escala 1/500 000. Serviços Geológicos de Portugal, Lisboa.
- Peck, R.E., 1938. A new family of Charophyta from the Lower Cretaceous of Texas. *Journal of Paleontology* 12, 285–304.
- Peck, R.E., 1941. Lower Cretaceous Rocky Mountain nonmarine microfossils. *Journal of Paleontology* 15, 285–304.
- Peck, R.E., 1957. North American Charophyta. Geological Survey Professional Paper 294A, pp. 1–44.
- Pereira, R., Cabral, M.C., 2005. Charophytes from the lower Aptian of Rio de Mouro (Lisbon region, Portugal). *Revista Espanola de Paleontologia* 37, 171–181.
- Pérez-Cano, J., 2021. The Barremian charophytes from the Maestrat Basin: taxonomy, palaeoecology, palaeobiogeography and biostratigraphy. (PhD Thesis). Universitat de Barcelona, p. 245.
- Pérez-Cano, J., Bover-Arnal, T., Martín-Closas, C., 2020. Barremian charophytes from the Maestrat Basin (Iberian Chain). *Cretaceous Research* 115, 104544.
- Pérez-Cano, J., Bover-Arnal, T., Martín-Closas, C., 2022a. Barremian–early Aptian charophyte biostratigraphy revisited. *Newsletters on Stratigraphy* 55 (2), 199–230.
- Pérez-Cano, J., Bover-Arnal, T., Martín-Closas, C., 2022b. Charophyte communities in Barremian Iberian wetlands. *Facies* 68, 13.
- Pia, J. von, 1927. Die Siphonae verticillatae vom Karbon bis zur Kreide. *Abhandlungen der zoologisch-botanischen Gesellschaft in Wien*, Band XI, Heft 2, 263.
- Pictet, A., Delanoy, G., Adatte, T., Spangenberg, J.E., Baudouin, C., Boselli, P., Kindler, P., Föllmi, K.B., 2015. Three successive phases of platform demise during the early Aptian and their association with the oceanic anoxic Selli episode (Arcèche, France). *Palaeogeography, Palaeoclimatology, Palaeoecology* 418, 101–125.
- Ramalho, M., Rey, J., 1981. Réflexions sur la formation crétacée de Porto de Mos (Algarve, Portugal). *Comunicações Geológicas* 67 (1), 35–39.
- Ramos, A., Fernández, O., Terrinha, P., Muñoz, J.A., 2016. Extension and inversion structures in the Tethys–Atlantic linkage zone, Algarve Basin, Portugal. *International Journal of Earth Sciences* 105, 1663–1679.
- Reboullet, S., Rawson, P.F., Moreno-Bedmar, J.A., Aguirre-Urreta, M.B., Barragán, R., Bogomolov, Y., Company, M., González-Arreola, C., Idakieva Stoyanova, V., Lukeneder, A., Matron, B., Mitta, V., Randrianaly, H., Vašíček, Z., Baraboshkin, E.J., Bert, D., Bersac, S., Bogdanova, T.N., Bulot, L.G., Latil, J.-L., Mikhailova, I.A., Ropolo, P., Szives, O., 2011. Report on the 4th International Meeting of the IUGS Lower Cretaceous Ammonite Working Group, the “Kilian Group” (Dijon, France, 30th August 2010). *Cretaceous Research* 32, 786–793.
- Reboullet, S., Szives, O., Aguirre-Urrea, B., Barragán, R., Company, M., Frau, C., Kakabadze, M.V., Klein, J., Moreno-Bedmar, J.A., Lukeneder, A., Pictet, A., Ploch, I., Raisossadat, S.N., Vašíček, Z., Baraboshkin, E.J., Mitta, V.V., 2018. Report on the 6th International Meeting of the IUGS Lower Cretaceous Ammonite Working Group, the Kilian Group (Vienna, Austria, 20th August 2017). *Cretaceous Research* 91, 100–110.
- Reid, C., Groves, J., 1916. Preliminary report on the Purbeck Characeae. *Proceedings of the Royal Society B* 89, 252–256.
- Rey, J., 1983. Le Crétacé de l'Algarve: Essai de Synthèse. *Comunicações dos Serviços Geológicos de Portugal* 69, 87–101.
- Rey, J., 1986. Micropaleontological assemblages, paleoenvironments and sedimentary evolution of Cretaceous deposits in the Algarve (southern Portugal). *Palaeogeography, Palaeoclimatology, Palaeoecology* 55, 233–246.
- Rey, J., 2006. Les formations Crétacées de l'Algarve Occidentale et Centrale. *Comunicações Geológicas* 93, 39–80.
- Rey, J., 2009. Les formations Crétacées de l'Algarve Oriental. *Comunicações Geológicas* 96, 19–38.
- Rey, J., Ramalho, M., 1974. Le Crétacé inférieur de l'Algarve occidentale (Portugal). *Comunicações dos Serviços Geológicos de Portugal* 57, 155–181.
- Riveline, J., Berger, J.P., Bilan, W., Feist, M., Martín-Closas, C., Schudack, M., Soulié-Märsche, I., 1996. European Mesozoic–Cenozoic Charophyte Biozonation. *Bulletin Société Géologique de France* 167, 453–468.
- Rocha, R., 1976. Estudo estratigráfico e paleontológico do Jurássico do Algarve ocidental. *Ciencias da Terra* 2, 178.
- Rocha, R., Marques, B., Antunes, M., Pais, J., 1989. Carta Geológica de Portugal na escala 1/50 000. Notícia explicativa da folha 52–B, Albufeira. Serviços Geológicos de Portugal, Lisboa.

- Sanjuan, J., Vicente, A., Pérez-Cano, J., Stoica, M., Martín-Closas, C., 2021. Early Cretaceous charophytes from south Dobrogea (Romania). *Biostratigraphy and palaeobiogeography*. *Cretaceous Research* 122, 104762.
- Schudack, M.E., 1986. Zur Nomenklatur der Gattungen *Porochara* Mädlér 1955 (syn *Musacchiella* Feist et Grambast-Fessard 1984) und *Feistiella* n. gen. (Charophyta). *Paläontologische Zeitschrift* 60, 21–27.
- Schudack, M.E., 1993. Die Charophyten im Oberjura und Unterkreide Westeuropas. Mit einer phylogenetischen Analyse der Gesamtgruppe. *Berl. Geowiss. Abh. (A)*, 8, 1–209.
- Smith, G.M., 1938. Botany, vol. I, Algae and Fungi. Charophyceae. McGraw Hill, New York, p. 127.
- Soulié-Marsche, I., 1994. The paleoecological implications of the charophyte flora of the Trinity Division, Junction, Texas. *Journal of Paleontology* 68, 1145–1157.
- Terrinha, P.A.G., 1998. Structural Geology and Tectonic Evolution of the Algarve Basin, South Portugal (Unpubl. PhD thesis). Imperial College London (University of London), p. 430.
- Terrinha, P., Rocha, R., Rey, J., Cachão, M., Moura, D., Roque, C., Martins, L., Valadares, V., Cabral, J., Azevedo, M.R., Barbero, L., Clavijo, E., Dias, R.P., Matias, H., Madeira, J., Silva, C.M., Munhá, J., Rebelo, L., Ribeiro, C., Vicente, J., Noiva, J., Youbi, N., Bensalah, M.K., 2013. A Bacia do Algarve: Estratigrafia, paleogeografia e tectónica. In: Dias, R., Araújo, A., Terrinha, P., Kullberg, J.C. (Eds.), *Geologia de Portugal, Geologia Meso-cenozóica de Portugal*, vol. II, pp. 29–166.
- Tibert, N.E., Colin, J.P., Kirkland, J.I., Alcalá, L., Martín-Closas, C., 2013. Lower Cretaceous nonmarine ostracodes from an Escucha Formation bonebed in eastern Spain. *Micropaleontology* 59, 83–91.
- Tiss, L., Trabelsi, K., Kamoun, F., Soussi, M., Houla, Y., Sames, B., Martín-Closas, C., 2019. Middle Jurassic charophytes from southern Tunisia: Implications on evolution and paleobiogeography. *Review of Palaeobotany and Palynology* 263, 65–84.
- Trabelsi, K., Soussi, M., Touir, J., Houla, Y., Abbes, C., Martín-Closas, C., 2016. Charophyte biostratigraphy of the non-marine lower cretaceous in the Central Tunisian Atlas (North Africa): palaeobiogeographic implications. *Cretaceous Research* 67, 66–83.
- Verati, C., Rapaille, C., Féraud, G., Marzoli, A., Bertrand, H., Youbi, N., 2007.  $^{40}\text{Ar}/^{39}\text{Ar}$  ages and duration of the Central Atlantic Magmatic Province volcanism in Morocco and Portugal and its relation to the Triassic-Jurassic boundary. *Palaeogeography, Palaeoclimatology, Palaeoecology* 344, 308–325.
- Vicente, A., Expósito, M., Sanjuan, J., Martín-Closas, C., 2016. Small sized charophyte gyrogonites in the Maastrichtian of Coll de Nargó, Eastern Pyrenees: An adaptation to temporary ponds. *Cretaceous Research* 57, 443–456.
- Vicente, A., Martín-Closas, C., 2013. Lower Cretaceous charophytes from the Seranía de Cuenca, Iberian chain: taxonomy, biostratigraphy and palaeoecology. *Cretaceous Research* 40, 227–242.
- Vilas-Boas, M., Paterson, N.W., Pereira, Z., Fernandes, P., Cirilli, S., 2022. The age of the first pulse of continental rifting associated with the breakup of Pangea in Southwest Iberia: new palynological evidence. *Journal of Iberian Geology* 48, 181–190.
- Wang, S., 1965. Mesozoic and Tertiary Charophyta from Jinquan basin of Kansu province. *Acta Palaeontologica Sinica* 13, 485–499.
- Wang, Z., Lu, H.N., 1982. Classification and evolution of Clavatoraceae with notes on its distribution in China. *Bulletin Nanjing Institute of Geology and Palaeontology, Academia Sinica* 4, 77–104 (in Chinese).
- Wissler, L., Funk, H., Weissert, H., 2003. Response of Early Cretaceous carbonate platforms to changes in atmospheric carbon dioxide levels. *Palaeogeography, Palaeoclimatology, Palaeoecology* 200, 187–205.

### Appendix 1. Specimens and provisional reference of each figured specimen.

Figure	Taxon	Sample	Ref. prov.	Ref. Museum
<b>Fig. 3</b>				
A and B	<i>Porochara</i> cf. <i>fusca</i>	C127W	Arr-Ch-1	
C	<i>Echinochara lazarii</i>	C152	Arr-Ch-2	
D	<i>Atopochara trivolvris</i> var. <i>triquetra</i>	C127W	Arr-Ch-3	
E and F	<i>Atopochara trivolvris</i> var. <i>triquetra</i>	C127W	Arr-Ch-4	
G	<i>Atopochara trivolvris</i> var. <i>triquetra</i>	C127W	Arr-Ch-5	
H	<i>Atopochara trivolvris</i> var. <i>triquetra</i>	C127W	Arr-Ch-6	
I	<i>Atopochara trivolvris</i> var. <i>trivolvris</i>	C127W	Arr-Ch-7	
J	<i>Atopochara trivolvris</i> var. <i>trivolvris</i>	C178	Arr-Ch-8	
K	<i>Atopochara trivolvris</i> var. <i>trivolvris</i>	C178	Arr-Ch-9	
L	<i>Atopochara trivolvris</i> var. <i>trivolvris</i>	C178	Arr-Ch-10	
M	<i>Atopochara trivolvris</i> var. <i>trivolvris</i>	C178	Arr-Ch-11	
N	<i>Atopochara trivolvris</i> var. <i>trivolvris</i>	C178	Arr-Ch-12	
O	<i>Atopochara trivolvris</i> var. <i>trivolvris</i>	C178	Arr-Ch-13	
P	<i>Atopochara trivolvris</i> var. <i>trivolvris</i>	C178	Arr-Ch-14	
<b>Fig. 4</b>				
A	<i>Clavator grovesii</i> var. <i>jiuquanensis</i>	C127W	Arr-Ch-15	
B	<i>Clavator grovesii</i> var. <i>jiuquanensis</i> adv.	C127E	Arr-Ch-16	
C	<i>Clavator grovesii</i> var. <i>jiuquanensis</i> adv.	C127E	Arr-Ch-17	
D	<i>Clavator grovesii</i> var. <i>jiuquanensis</i> adv.	C127W	Arr-Ch-18	
E	<i>Clavator grovesii</i> var. <i>jiuquanensis</i>	C127W	Arr-Ch-19	
F	<i>Clavator grovesii</i> var. <i>jiuquanensis</i>	C127W	Arr-Ch-20	
G	<i>Clavator grovesii</i> var. <i>corrugatus</i>	C178	Arr-Ch-21	
H	<i>Clavator grovesii</i> var. <i>corrugatus</i>	C178	Arr-Ch-22	
I	<i>Clavator grovesii</i> var. <i>corrugatus</i>	C178	Arr-Ch-23	
J	<i>Clavator grovesii</i> var. <i>corrugatus</i>	C178	Arr-Ch-24	
K	<i>Clavator grovesii</i> var. <i>corrugatus</i>	C178	Arr-Ch-25	
L	<i>Clavator grovesii</i> var. <i>corrugatus</i>	C178	Arr-Ch-26	
M	<i>Clavator harrisii</i> var. <i>harrisii</i>	C127	Arr-Ch-27	
N	<i>Clavator harrisii</i> var. <i>harrisii</i>	C127	Arr-Ch-28	
O	<i>Clavator harrisii</i> var. <i>harrisii</i>	C127	Arr-Ch-29	
P	<i>Clavator harrisii</i> var. <i>reyi</i>	C32	Arr-Ch-30	
Q	<i>Clavator harrisii</i> var. <i>reyi</i>	C178	Arr-Ch-31	
R	<i>Clavator harrisii</i> var. <i>zavialensis</i> primitive	C178	Arr-Ch-32	
S	<i>Clavator harrisii</i> var. <i>zavialensis</i>	C178	Arr-Ch-33	
T	<i>Clavator harrisii</i> var. <i>zavialensis</i>	C178	Arr-Ch-34	
U	<i>Munieria grambastii</i>	C127W	Arr-Ch-35	
V	<i>Munieria grambastii</i>	C127W	Arr-Ch-36	
W	<i>Clavatorax</i> sp.	C127W	Arr-Ch-37	



## Appendix 2. Distribution of the charophyte taxa in the studied samples.

### Supplementary material 1

The number of charophyte fructifications found in each sample of the Arrifes section.

	Samples						
	C32	C127W	C127E	C152	C178	C182	C199
Porocharaceae							
<i>Porochara</i> cf. <i>fusca</i> .		5					
Clavatoraceae							
Atopocharoidae							
<i>Echinochara lazarii</i>				15			
<i>Atopochara trivolv</i> is var. <i>triquetra</i>	2	15	3	1			
<i>Atopochara trivolv</i> is var. <i>trivolv</i> is		60			231	9	
Clavatoroidae							
<i>Clavator grovesii</i> var. <i>jiuquanensis</i>	10	27	76				
<i>Clavator grovesii</i> var. <i>corrugatus</i>		2	9		327	18	4
<i>Clavator harrisii</i> var. <i>harrisii</i>	1	24	5		3		
<i>Clavator harrisii</i> var. <i>reyi</i>	5	20	48		53	1	
<i>Clavator harrisii</i> var. <i>zavialensis</i>		124	64		220	7	

## Appendix 3. Comparison of the described herein upper Barremian–Lower Aptian biostratigraphy with Riveline et al. (1996), and Pérez-Cano et al. (2022a).

		Ammonite biozones	Dinoflagellate biozones	Charophyte biozones				
		Reboulet et al. 2018	Lereeveld 1995, 1997	Riveline et al., 1996	Pérez Cano et al. 2022a		This study	
					European	Eurasian	European	Eurasian
Aptian	Upper	<i>Hypacanthoplites jacobi</i>	<i>Cribroperidinium tenuiceras</i>	<i>Clavator grovesii</i> var. <i>lusitanicus</i>	<i>Clavator grovesii</i> var. <i>lusitanicus</i>		<i>Clavator grovesii</i> var. <i>corrugatus</i>	
		<i>Acanthohoplites nolani</i>						
		<i>Parahoplites melchioris</i>						
		<i>Epicheloniceras martini</i>						
	Lower	<i>Dufrenoyia furcata</i>	<i>Odontochitina operculata</i>	<i>Asciidiella cruciata</i>	<i>Asciidiella cruciata</i> - <i>Pseudoglobator paucibracteatus</i>	<i>Clavator grovesii</i> var. <i>jiuquanensis</i>		
<i>Deshayesites deshayesi</i>								
<i>Deshayesites forbesi</i>								
<i>Deshayesites ogilvensis</i>								
<i>Martelites sarasini</i>								
<i>Imerites giraudi</i>								
Barremian	Upper	<i>Gerhardia sartousiana</i>	<i>Subtilisphaera scabrata</i>				<i>Asciidiella cruciata</i> - <i>Pseudoglobator paucibracteatus</i>	<i>Clavator grovesii</i> var. <i>jiuquanensis</i>
		<i>Toxancyloceras vanderheckii</i>						